

Simulation of nanodiamond and nanographite formation from molten carbon in the presence of hydrogen

A. Sorkin, Joan Adler,* and R. Kalish

Department of Physics, Technion, Israel Institute of Technology, Haifa 32000, Israel

(Received 11 February 2008)

Hydrogen plays a significant role in the formation of nanodiamond, terminating diamond surfaces, and removing sp^2 -bonded atoms from the surface during chemical-vapor deposition diamond growth. However, there are only few calculations that simulate nanodiamond development directly and even less that do so in a hydrogen-containing environment. Recently, nanoscale graphitic layers embedded in amorphous carbon were observed experimentally. We report here on results from a comprehensive study of nanodiamond and nanographite formation from molten carbon in the presence of hydrogen under varied conditions of external pressure and cooling rate. We find that hydrogen-free nanodiamond crystals are precipitated more readily at increased melt densities and cooling rates, whereas slower cooling rates permit formation of graphitic layers.

DOI: XXXX

PACS number(s): 62.50.–p, 81.05.Uw, 61.43.Bn

I. INTRODUCTION

A carbon atom can bond to another C atom with different bonding configurations including sp^2 , which is the bonding in graphite and sp^3 , as what occurs in diamond.¹ Carbon can also form amorphous structures (denoted by a-C), in which the bonding can be predominantly sp^2 (graphitelike), sp^3 (diamondlike), or a mixture of both. The extremely different physical and chemical properties of diamond and graphite are also reflected in their amorphous forms. Diamondlike amorphous carbon (DLC) in which the C atoms are predominantly tetrahedrally (sp^3) bonded is denoted as ta-C and possesses many of the very attractive properties of diamond. Therefore it is a material of great technological importance.

Hydrogen readily bonds to C, giving rise to an enormous variety of molecules which are the building blocks of organic chemistry. When hydrogen is present in the various forms of amorphous carbon, it forms amorphous hydrogenated carbon, which is denoted by a-C:H. The properties of a-C and a-C:H materials, theories of formation and structure as well as their production, have recently been reviewed by Robertson.²

Hydrogen can also be present in crystalline diamond, occupying interstitial positions—the locations of which are still under dispute.³ Hydrogen on a diamond surface gives rise to a negative electron affinity and other interesting properties.⁴ The presence of hydrogen could reduce the gap in the density of states in amorphous diamond.⁵ Hydrogen is an essential ingredient for the growth of diamond by chemical-vapor deposition (CVD) methods, as the abundant (usually more than 95%) presence of hydrogen in the C-containing growth plasma is necessary for the growth of high-quality diamond. It is believed that the role of (atomic) hydrogen during CVD diamond growth is to remove undesired sp^2 bonded atoms from the growth surface and assist the crystal formation by saturating the dangling C surface bonds.

An interesting question, which is addressed here, is whether the presence of hydrogen in molten amorphous carbon also assists the formation of diamond crystallites during the cooling of the liquid. In other words, would a material that might solidify as hydrogen-containing tetrahedral carbon

also contain some diamond crystallites? The subnanodiamond grains may serve as nucleation centers for further diamond growth as predicted and described by the subimplantation model of Lifshitz *et al.*^{6,7} This model was developed for hydrogen-free amorphous carbon layers formed during high-dose low-energy C ion implantation. Michaelson and Hoffman⁸ provided experimental evidence for this mechanistic model.

In this paper, we describe our studies of the structural and electronic properties of hydrogenated amorphous carbon networks generated with different densities and cooling rates, and with different contents of hydrogen atoms with tight-binding molecular-dynamics (MD) simulations. We found that hydrogen-free nanodiamond crystals were formed within the compressed hydrogenated amorphous matrix; the hydrogen atoms are being expelled from these diamond clusters. The probability of precipitation of diamond clusters increases with increasing density and cooling rates, and slightly decreases with hydrogen content. The orientations of the diamond clusters were found to be random. The possibility of transforming amorphous carbon into oriented graphitic planes has recently been described.⁹ For slower cooling rates we indeed observed such layers in visualizations of our simulated samples under certain conditions.

II. COMPUTATIONAL INTRODUCTION

Many authors have simulated the structure of pure or hydrogenated amorphous carbon networks that were generated under conditions close to those occurring within the “thermal spike.”^{6,10–16} Most of these, except in Refs. 15 and 16, did not involve external pressure. Only a few observed a nucleation of diamond. For example, Kopidakis *et al.*¹⁰ investigated the structures of hydrogenated amorphous carbon networks by orthogonal tight-binding molecular-dynamics simulations. They found that hydrogen tends to break carbon-carbon bonds in tetrahedral amorphous carbon, ta-C. This reduction in C-C coordination makes ta-C softer and induces more electronic states in the energy-band gap region. As can be seen from our description below the conditions of their simulations were very similar to those reported in our

95 study. However, in contrast to our findings, which clearly
96 show nanodiamonds embedded in the amorphous matrix, the
97 authors of Ref. 10 did not identify any ordered sp^3 clusters in
98 their samples.

99 Ofer *et al.*¹¹ simulated a hydrogenated amorphous carbon
AQ: #00 or diamond composite with a tight-binding method. They
2 101 found that the total fraction of sp^3 -bonded carbon atoms was
102 not a monotonic function of hydrogen concentration. As the
103 number of H atoms increases, the number of sp^3 bonds also
104 increases until the saturation of H was achieved and a de-
105 crease in the number of sp^3 bonds began. In their visualiza-
106 tions one can see that the new sp^3 bonds form near previ-
107 ously formed sp^3 bonds, which suggest growth of a diamond
108 cluster.

109 Kohary *et al.*¹² simulated the ion bombardment process
110 during bias-enhanced nucleation (BEN) by the nonortho-
111 gonal tight-binding method. A heated a-C:H layer was bom-
112 barded with methyl and acetylene ions of different energies.
113 The bombardment caused structural rearrangement in the
114 substrate resulting in an increase in the total sp^3 content in
115 the film, while the total sp^2 content is decreased by the same
116 magnitude. No formation of diamond nuclei or aligned gra-
117 phitic planes was observed. The nonorthogonal tight-binding
118 simulations of the first stage of diamond nucleation process
119 in a dense amorphous hydrogenated carbon that was carried
120 out by Lifshitz *et al.*⁶ showed that a diamondlike sp^3 cluster
121 could spontaneously form in a hydrogenated amorphous car-
122 bon network (25% of hydrogen atoms) generated at a density
123 of 3 g/cc. The hydrogen was concentrated in the more porous
124 parts of the cell and decorated the surface of the sp^3 clusters,
125 mainly forming sp^3 C-H bonds.

126 In a previous paper¹⁵ we studied the nucleation of dia-
127 mond from liquid carbon without hydrogen under extreme
128 pressures. We observed the formation of large diamond crys-
129 tallites in an amorphous carbon network generated at densi-
130 ties of 3.5–3.9 g/cc and fast cooling rates (1000 K/ps). We
131 found that the probability of precipitation of diamond crys-
132 tallites increases with density and with cooling rate. At
133 slower cooling rates (200–500 K/ps), some samples trans-
134 formed to graphite.

135 The conditions of the Ref. 15 simulations, which describe
136 solidification of hydrogen-free liquid C, are very similar to
137 those of Wang *et al.*,¹⁶ who investigated the structure of
138 amorphous carbon over a wide range of densities (from 2.2
139 to 4.4 g/cc) that are generated by rapid quenching of liquid
140 carbon phase by the same method. The authors did not iden-
141 tify any ordered sp^3 clusters in their samples. We note two
142 reasons for this discrepancy: first, the precipitation of dia-
143 mond clusters is a random process, and if the number of
144 realizations is small, the probability of generating an amor-
145 phous carbon sample with a crystalline diamond cluster
AQ: #46 within is not large. The statistics of Wang *et al.*¹⁶ could be
3 147 insufficient to identify large diamond crystallites in their
148 samples. The second reason is that it is difficult to identify a
149 small diamond crystallite in a large amorphous sp^3 -bonded
150 carbon network without modern visualization tools. One
151 such tool is our atomic visualization (AViz) (Ref. 17) pack-
152 age which possesses all the capabilities needed to identify
153 diamond clusters.

154 Fast quenching of a compressed hydrogenated liquid car-
155 bon sample, similar to that occurring during the BEN pro-

cess, is possibly the laboratory system closest to our simula- 156
tions. The times available to perform MD computations (a 157
few picoseconds) and the sample sizes (containing a few 158
hundred atoms) are similar to those of the thermal spike. The 159
densities at which our simulations were carried out (3.5 and 160
3.9 g/cc) can reasonably be locally attained within the ther- 161
mal spike. The hydrogen content in our samples does not 162
exceed 10%, while the optimal hydrogen concentration for 163
diamond nucleation in an a-C:H matrix during BEN is 25%.⁶ 164
The reason for such a low hydrogen content in our calcula- 165
tions is that no liquid carbon with a high hydrogen content 166
could be obtained perhaps because the velocities of the mov- 167
ing hydrogen atoms are so much higher than those of carbon 168
atoms. The temperatures required in order to melt carbon are 169
6000–8000 K. At these temperatures the velocity of hydro- 170
gen atoms is so high that our tight-binding code is capable of 171
only treating a few hydrogen atoms without collapse of the 172
sample. 173

174 Because of the low probability of nucleationlike phenom- 174
ena, relatively long simulations of relatively large systems 175
are needed. Such simulations are not realistic with *ab initio* 176
methods. In this respect, tight-binding simulations, such as 177
ours, are a reasonable compromise between accurate but 178
slow *ab initio* calculations and calculations with empirical 179
potentials, which are fast but do not ensure sufficient accu- 180
racy. Reliability of tight-binding molecular dynamics^{16,18} as 181
well as the effects of small sample sizes were discussed by 182
us previously.¹⁵ 183

III. DETAILS OF THE SIMULATIONS 184

185 Our calculations were carried out at constant volume 185
(density). Periodic boundary conditions were applied to the 186
samples in all three directions. In order to describe the inter- 187
actions between carbon atoms we used the tight-binding 188
model¹⁸ of the OXON package.¹⁹ The electron wave functions 189
were expanded in terms of a basis set of valence electron 190
wave functions, controlling the attractive part of the poten- 191
tial, while the repulsive one was treated empirically. The 192
 Γ -point Brillouin-zone sampling was used for the electronic 193
calculations and the MD step was 1×10^{-15} s. Visualization 194
with the AViz (Ref. 17) was applied to identify diamond 195
clusters as mentioned above. 196

197 The samples used in the simulations were initially ar- 197
ranged as a perfect diamond crystal of a size $3 \times 3 \times 3$ unit 198
cells (i.e., 216 carbon atoms) with a density of 3.5 g/cc (i.e., 199

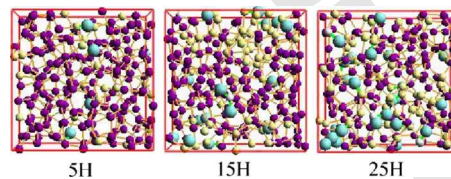


FIG. 1. (Color online) A-C:H structures with different content of 199
hydrogen atoms. The black, gray, and white balls (purple, yellow, 200
and white online) are the carbon atoms with four, three, and two 201
C-C bonds (excluding C-H bonds), respectively. Hydrogen atoms 202
are represented by large gray (light blue online) balls. 203

TABLE I. Average number (rounded to nearest integer) of differently bonded carbon atoms in the a-C:H samples generated at 3.9 g/cc and with a cooling rate of 1000 K/ps.

Number of H atoms in the a-C:H sample	0	5	10	15	25
Number of C atoms with four C-C and zero C-H bonds	190	186	172	150	151
Number of C atoms with three C-C and zero C-H bonds	24	22	32	47	31
Number of C atoms with two C-C and zero C-H bonds	2	3	2	4	5
Number of C atoms with four C-C and one C-H bonds	0	0	0	0	2
Number of C atoms with three C-C and one C-H bonds	0	5	9	13	21
Number of C atoms with three C-C and two C-H bonds	0	0	0	0	1
Number of C atoms with two C-C and one C-H bonds	0	0	1	2	4
Number of C atoms with two C-C and two C-H bonds	0	0	0	0	1
Total number of sp^3 -bonded C atoms	190	191	181	163	172
Total number of sp^2 -bonded C atoms	24	22	33	49	35
Total number of sp -bonded C atoms	2	3	2	4	5

the sides of simulation box were 10.65 Å). The diamond was melted at a temperature of 8000 K during 5, 10, 15, 20, and 25 ps. These five liquid carbon samples were rapidly cooled with a cooling rate of 500 K/ps. In order to generate samples of amorphous carbon with a higher density, each of the configurations was isotropically compressed by changing the volume of the unit cell to the densities of 3.9 g/cc (the length of simulation box was decreased up to 10.3 Å). We then placed 5–25 hydrogen atoms in each sample at both densities (3.5 and 3.9 g/cc). Pairs of neighboring bonded carbon atoms were randomly chosen, and the hydrogen atoms were positioned at the midpoint of the bond between them. The volume of the simulation box remained unchanged; hence, the resulting density of the sample slightly increases as the number of H atoms increases. Then the hydrogenated samples were repeatedly heated up to 6000 K and cooled to room temperature with three different cooling rates: fast (1000 K/ps), intermediate (500 K/ps), and slow (200 K/ps). In total, 120 simulations were carried out.

The entire computational effort of all the calculations for the many different cases, careful sample preparations, ad-

equate statistics, and equilibration was substantial. Several fast Pentium workstations, each with several gigabyte of random access memory (RAM), were used for more than one year. We have found OXON (Ref. 19) to be a very helpful tool for efficient tight-binding simulations, but even for our sample sizes the computations were memory limited as well as being time limited. For the present project the sample sizes and boundary conditions used are indeed adequate for the thermal spike type of phenomena that we are researching here. This would, however, not be the case if we were to concern ourselves with interfaces between distinct carbon allotropes.

IV. RESULTS

A. Structure of hydrogenated amorphous carbon

Typical structures of the a-C:H samples generated at the initial density of 3.9 g/cc with the fast cooling rate (1000 K/ps) and with different content of hydrogen atoms are presented in Fig. 1. Averages of the detailed counts of differently bonded atoms as a function of hydrogen concentration

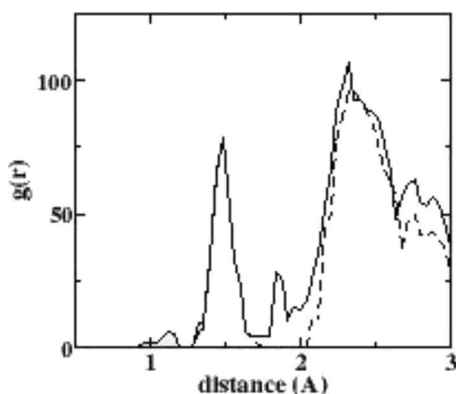


FIG. 2. Radial distribution function of the hydrogenated amorphous carbons containing 25 hydrogen atoms generated at 3.9 g/cc with the intermediate cooling rate (solid line) compared with that for C-C bonds only (dashed line). Additional peaks of the complete radial distribution located at ~ 1.13 and ~ 1.86 Å represent the distances from H atoms to nearest and second-nearest carbon atoms, respectively.

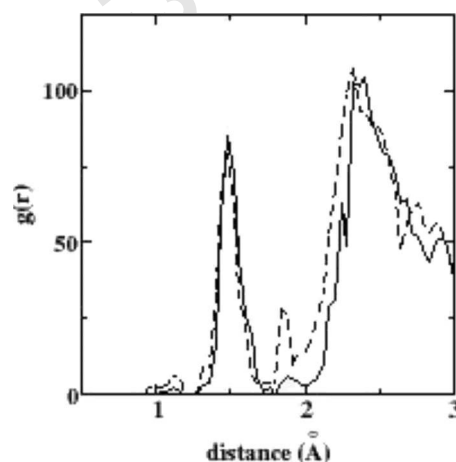


FIG. 3. Radial distribution function of the hydrogenated amorphous carbon samples generated at 3.9 g/cc containing 5 hydrogen atoms (solid line) and containing 25 hydrogen atoms (dashed line).

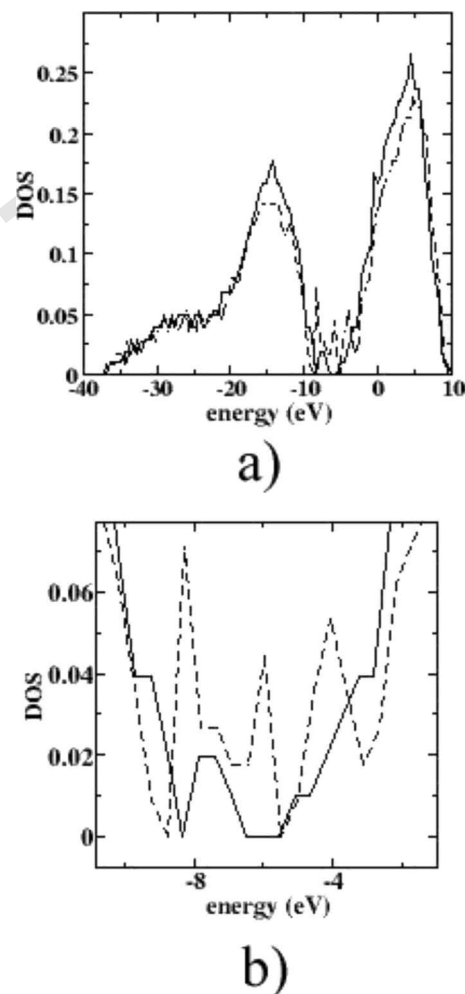


FIG. 4. (a) Density of states of the hydrogenated amorphous carbon samples at 3.9 g/cc, containing 5 hydrogen atoms (solid line) and 25 hydrogen atoms (dashed line). In (b) a magnified part of the density of states near the band gap is shown.

TABLE II. Band gap of the samples prepared at 3.9 g/cc with the fast cooling rate.

Number of H atoms	sp^3 fraction (%)	Band gap (eV)
0	82–90	1.3–3.7
5	80–88	0.3–1
10	80–85	0

atoms there are 150–151 such atoms. At the same time the average number of carbon atoms with three carbon neighbors and a single hydrogen neighbor increases from 5 to 21 as the number of hydrogen atoms is increased from 5 to 25. It is clear that the hydrogen atoms break the C-C bonds and replace carbon atoms. The total fraction of sp^3 -bonded atoms (C atoms with four C-C bonds, C atoms with three C-C and one C-H bonds, and C atoms with two C-C and two C-H bonds) appears to decrease with hydrogen concentration within our accuracy for this case of initial density (3.9 g/cc) and fast cooling rate. Only a few fivefold carbon (C with four C-C and one C-H bonds, and C with three C-C and two C-H bonds) atoms were found, appearing only in the samples with 25 hydrogen atoms. (The slight nonmonotonicities are probably indicative of our statistical errors, but we cannot exclude a connection with the fivefold atoms for the case with the highest number of hydrogen atoms.)

The radial distribution function of the sample containing 25 hydrogen atoms is shown in Fig. 2. On the same figure we draw the partial radial distribution function of C-C bonds only. The complete radial distribution function has two low additional peaks located at ~ 1.13 and ~ 1.86 Å, which are the distances from H atoms to the nearest and next-nearest carbon atoms, respectively. The high peaks located at 1.52 and 2.4 Å represent the nearest carbon neighbors and next-nearest carbon neighbors for carbon atoms. We did not find any detectable dependence of C-C and C-H bond lengths on the number of hydrogen atoms in the samples within our range of hydrogen content. The average C-C and average C-H bond lengths were equal for all hydrogenated amorphous carbon samples generated at 3.9 g/cc and at the fast cooling rate (1.13 Å). This can be observed in Fig. 3, where the radial distribution functions of the hydrogenated amorphous carbon containing 5 and 25 hydrogen atoms are presented.

in these samples are listed in Table I. It is clearly seen that the increase in hydrogen atom content systematically reduces the number of sp^3 -bonded carbon atoms with four carbon neighbors.

For example, in the samples with five hydrogen atoms there are, on average, 186 fourfold carbon atoms with four carbon neighbors, while in the sample with 15–25 hydrogen

TABLE III. Number of carbon atoms with four C-C bonds (sp^3) or indication of the formation of nanographitic crystallites in the samples with 0, 5, or 25 hydrogen atoms generated with different densities and different cooling rates.

Number of H atoms	Density (g/cc)	Cooling rate		
		Fast	Intermediate	Slow
0	3.5	73,69,76,74,67	76,77,graphite,66,80	64,66,graphite,graphite,75
0	3.9	89,88,82,90,89,85	89,84,85,89,92	graphite,77,51,74,graphite
5	3.5	68,77,63,71,71	69,68,graphite,61,58	73,74,67,graphite,65
5	3.9	83,80,88,86,86	80,90,77,80,86	78,85,57,88,82
25	3.5	51,54,67,62,57	51,61,61,56,51	67,graphite,49,53,graphite
25	3.9	70,73,67,69,67	71,72,68,69,71	75,71,67,73,70,graphite

TABLE IV. Number of samples where diamond clusters containing more than ten atoms were found from sets of five samples generated at high density (3.9 g/cc).

Number of H atoms	Fast	Intermediate	Slow
0	4	1	1
5	1	2	0
10	1	1	0
15	1	0	1
25	0	2	0

282 The density of states of the samples generated at 3.9 g/cc
 283 with fast cooling rate is shown in Fig. 4 for different num-
 284 bers of hydrogen atoms. The presence of hydrogen decreases
 285 the band gap. For example, without hydrogen, an amorphous
 286 carbon sample with 90% of sp^3 -coordinated atoms shows a
 287 band gap of 3.7 eV, while the band gap of the hydrogenated
 288 amorphous carbon with five hydrogen atoms and 86% of
 289 sp^3 -bonded carbon atoms is 1 eV only. The reduction in the
 290 band gap with the increasing content of hydrogen is shown
 291 in Table II. The samples with 10–25 hydrogen atoms did not
 292 show any band gap.

293 We explored the influence of different cooling rates and
 294 different densities on the structure of the hydrogenated amor-
 295 phous carbon samples. In Table III we show the fraction of
 296 carbon atoms with four C-C bonds (sp^3) in the samples with
 297 5 and 25 hydrogen atoms that are generated with different
 298 densities and different cooling rates—each for five different
 299 samples. As in the case of amorphous carbon without
 300 hydrogen¹⁵ the fraction of sp^3 -bonded atoms decreases as the
 301 density decreases. A systematic influence of cooling rate on
 302 sp^3 content was not found. It should be noted that for inter-
 303 mediate and slow cooling rates some graphitic structures
 304 were identified, as will be discussed below.

305 B. Diamond nucleation in the hydrogenated carbon network

306 Most of the structures formed were highly inhomoge-
 307 neous and contained large sp^3 clusters that do not include
 308 hydrogen. Hydrogen seems to escape from these pure sp^3
 309 clusters. This sp^3 clustering signifies the initial stage of dia-
 310 mond cluster formation; some of the sp^3 clusters generated
 311 within our hydrogenated amorphous carbon samples clearly
 312 show a diamond structure. The clusters appeared in at least

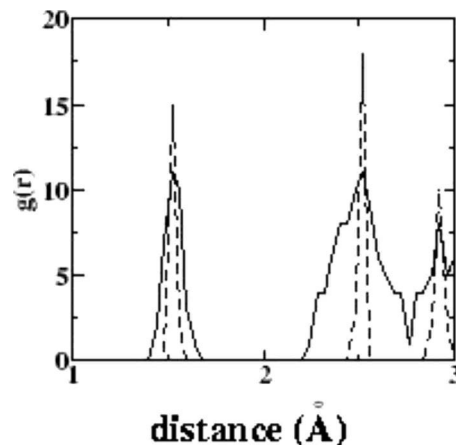


FIG. 6. Radial distribution function of a diamond cluster inside hydrogenated amorphous carbon, containing ten hydrogen atoms generated with intermediate cooling rate (solid line), compared with the radial distribution function of pure diamond (dashed line).

one case in each row (number of hydrogen atoms) of our
 summary in Table IV, where we list the number of diamond
 clusters containing more than ten atoms for samples gener-
 ated with the initial density of 3.9 g/cc for all cooling rates.
 From Table IV we conclude that the probability of diamond
 nucleation at fast and intermediate cooling rates appears to
 be slightly higher than at slow cooling rate. The dependence
 of the diamond nucleation on hydrogen content is not com-
 pletely monotonic. When no hydrogen atoms were inserted,
 fast cooling rates led to many large clusters at high density.
 At the low density of 3.5 g/cc we found only two cases
 where the sp^3 cluster had an ordered diamond structure: in
 the sample with five hydrogen atoms at intermediate cooling
 rate and in the sample with ten hydrogen atoms at fast cool-
 ing rate.

The best large diamond cluster was found in the sample
 generated at intermediate (500 K/ps) cooling rate within the
 sample with ten hydrogen atoms that are generated with high
 initial density (3.9 g/cc). This diamond cluster, shown in Fig.
 5 and viewed from different angles, is free from hydrogen
 atoms. The orientation of the diamond clusters relative to the
 walls of the simulation box was found to be arbitrary.

The obtained nanodiamonds were investigated by per-
 forming statistical analysis of their radial and angular distri-
 bution functions, as shown in Figs. 6 and 7. The first peak of
 the radial distribution function is located at 1.53 Å, which is
 very close to that of diamond, 1.54 Å. The peak of the an-

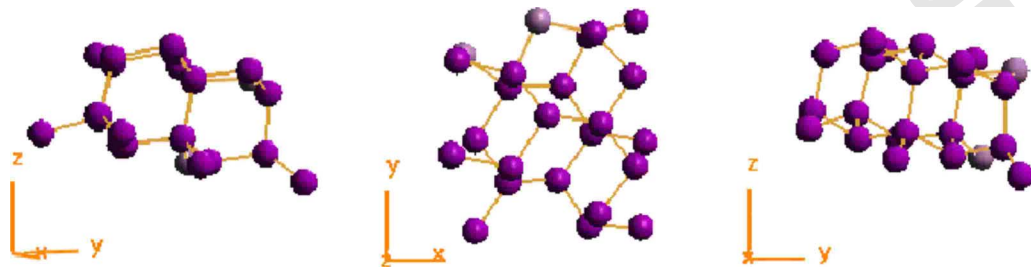


FIG. 5. (Color online) A diamond cluster containing 22 carbon atoms found in the sample with 10 hydrogen atoms that are generated at intermediate cooling rate.

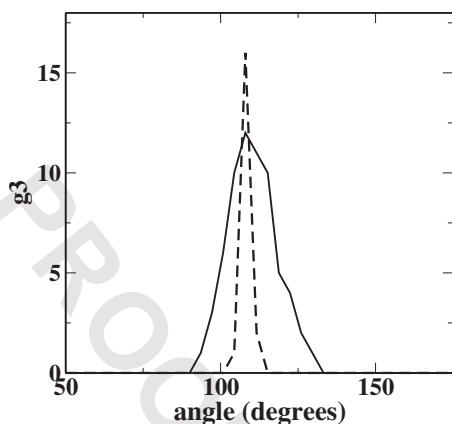


FIG. 7. Angular distribution function of diamond cluster inside hydrogenated amorphous carbon, containing ten hydrogen atoms generated at 3.9 g/cc with fast cooling rate (solid line), compared with the angular distribution function of pure diamond (dashed line).

340 gular distribution function is located at 111° , which is also
 341 close to the diamond peak at 109° . The density of states
 342 inside this cluster (see Fig. 8) shows a band gap of ~ 4 eV,
 343 which is slightly narrower than the band gap of perfect dia-
 344 mond at 3.5 g/cc with 5.4 eV.

345 C. Nanographitic crystallites

346 A number of samples generated at intermediate (500
 347 K/ps) and slow cooling rates (200 K/ps) exhibited clear for-
 348 mation of nanographitic crystallites, one such case is shown
 349 in Fig. 9. Note that not all the planes have a perfect graphitic
 350 structure. In Table III such graphitic configurations are listed,
 351 and we note that they did not form more than twice in each
 352 set of five samples. These graphitic configurations appeared
 353 more frequently at low density (3.5 g/cc) and for the slowest
 354 cooling rates. The orientation of the graphitic planes was
 355 random.

356 The radial distribution function of an entire sample (25
 357 hydrogen atoms generated at 3.9g/cc at a slow cooling rate),

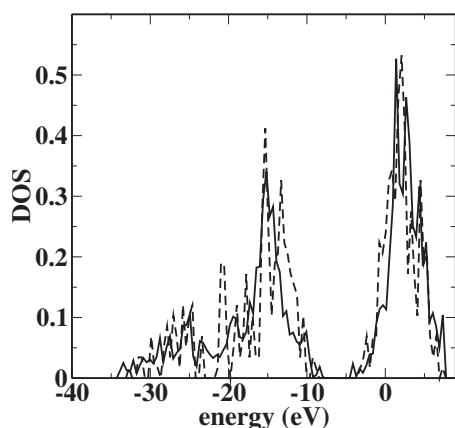


FIG. 8. Density of states of diamond cluster inside hydrogenated amorphous carbon, containing ten hydrogen atoms generated at 3.9 g/cc with intermediate cooling rate (solid line), compared with the density of states of pure diamond (dashed line).

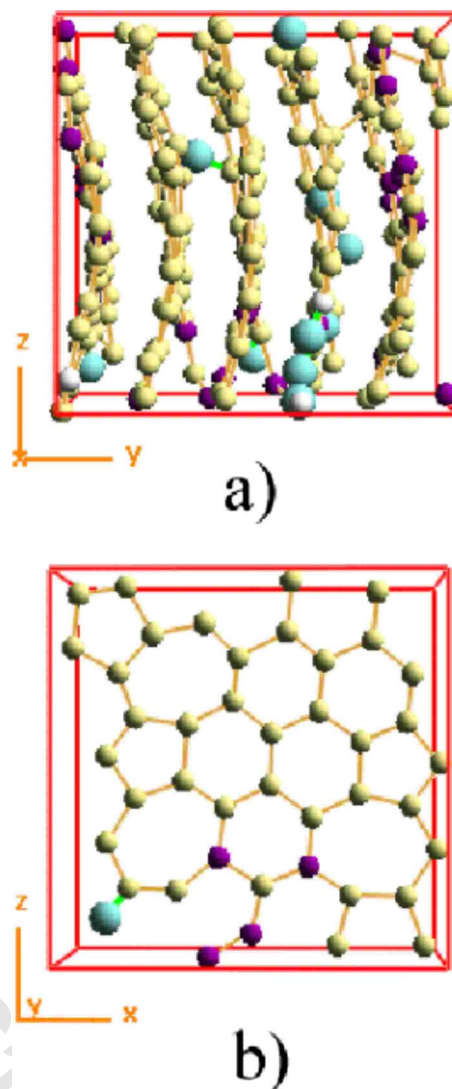


FIG. 9. (Color online) (a) A graphitic configuration containing ten hydrogen atoms generated at 3.9 g/cc with slow cooling rate. (b) A single damaged graphene sheet. Color coded as in Fig. 1.

in which graphitic sheets were obtained, is compared with 358
 that for C-C bonds only—shown in Fig. 10. The average C-H 359 AQ
 bond length in the graphitic configurations varied from 360 #6
 ~ 1.02 to ~ 1.1 Å, as the density decreases from 3.9 to 3.5 361
 g/cc. The interplanar distance is shorter than that of perfect 362
 graphite: 2.1 and 2.5 Å for the samples generated at 3.9 and 363
 3.5 g/cc, respectively; however, the present densities are 364
 much higher than those of perfect graphite (2.2 g/cc). The 365
 peak of the angular distribution function of the graphitic con- 366
 figuration, while broader than that of perfect graphite, is also 367
 located around 120° (see Fig. 11) which is the angle between 368
 two C atoms in perfect graphite. 369

V. SUMMARY

We have simulated precipitation of diamond and graphitic 371
 crystallites in compressed hydrogenated amorphous carbon 372
 samples generated by rapid quenching of liquid carbon. The 373
 hydrogen content of the samples as well as the pressure (den- 374

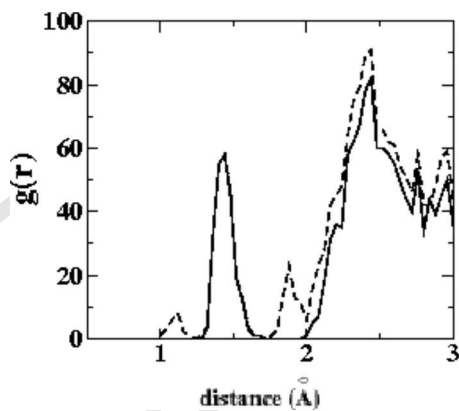


FIG. 10. Radial distribution function of hydrogenated graphite containing 25 hydrogen atoms generated at 3.9 g/cc with the slow cooling rate (dashed line) compared with the partial radial distribution function of C-C bonds only (solid line).

sity) and cooling rates were varied. Most of the samples generated in this way contained ta-C:H, i.e., were mostly sp^3 bonded. The hydrogen atoms bonded mainly with carbon atoms that have three carbon neighbors. The number of carbon atoms with four carbon neighbors decreases as the hydrogen content increases, while the total number of sp^3 -coordinated carbon atoms increases but was not a monotonic function of hydrogen concentration. The average length of the C-H bond was found to be 1.13 Å, which is slightly longer than the C-H distance in methane (1.09 Å). The increase in hydrogen content leads to a reduction in the band

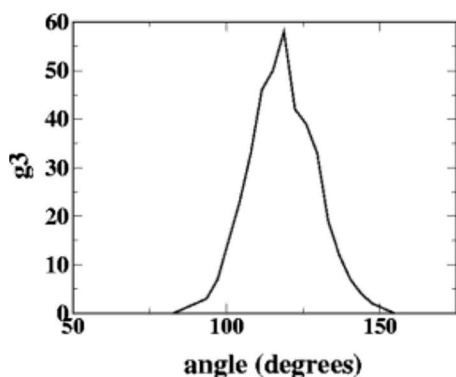


FIG. 11. Angular distribution function of hydrogenated graphite containing 25 hydrogen atoms generated at 3.9 g/cc with the slow cooling rate.

gap in our samples; the band gap disappeared for more than ten hydrogen atoms. This is due to the increase in the number of sp^2 -bonded carbon atoms.

All the samples, whose final phase was amorphous, contained large pure sp^3 clusters from which the hydrogen atoms had been expelled. Some of these sp^3 clusters could be identified as nanodiamond crystallites. The AViz (Ref. 17), which we used in this work, helped to identify the diamond clusters. The probability of precipitation of diamond crystallites in our simulations increases as the density is increased, and cooling rate increases independently of the hydrogen content. These trends are in qualitative agreement with experimental results of the bias-enhanced nucleation picture⁶ and also with the trends observed in detonation diamond nucleation,²⁰ where increasing pressure (density) and faster cooling rates lead to a higher diamond fraction in the detonation soot. The diamond clusters generated inside hydrogenated amorphous carbon network are smaller and of poorer quality than those formed without hydrogen atoms in our previous paper.¹⁵ This is in disagreement with the experimental results of Lifshitz *et al.*,⁶ who argued that the probability of diamond nucleation in hydrogenated matrix is higher. However the conditions of our simulations (range of densities and hydrogen contents) differed from those in the experiments of Lifshitz *et al.*⁶

At slow cooling rates graphitic configurations appeared in both hydrogenated and pure carbon samples. The probability of formation of these graphitic configurations decreases as the cooling rate and density increase and is independent of hydrogen content. As explained in the experimental study of Titov *et al.*²⁰ during the cooling process, the system passes through a pressure-temperature region in the carbon phase diagram where the graphitic phase is preferable. Therefore as the time spent in this region increases (cooling rate decreases) the probability of the formation of graphite increases.

These are simulations of nucleation of nanodiamond and nanographite crystallites in the presence of hydrogen from a totally disordered compressed liquid phase. The results support the model of diamond nucleation induced by energetic species that was proposed by Lifshitz *et al.*,⁶ where pure sp^3 clusters could precipitate in amorphous hydrogenated carbon formed on a substrate via a subplantation process and the experimental observation of nanographitic crystallites.⁹

ACKNOWLEDGMENTS

We are grateful to Y. Lifshitz and A. Hoffman for useful discussions. We thank A. Horsfield and M. Finnis for providing us with the OXON package.

434
435
436

*phr76ja@technion.ac.il

¹Hugh O. Pierson, *Handbook of Carbon, Graphite and Fullerenes* (Noyes, New Jersey, 1993).

²J. Robertson, *Mater. Sci. Eng.*, R. **37**, 129 (2002).

³D. Saada, J. Adler, and R. Kalish, *Phys. Rev. B* **61**, 10711 (2000).

⁴C. E. Nebel and J. Ristein, *Thin Film Diamond I*, Semiconductor

Science and Semimetals Vol. 76 (Elsevier, New York, 2003).

⁵D. P. Erchak, A. G. Ulyashin, R. B. Gelfand, N. M. Penina, A. M. Zaitsev, V. S. Varichenko, V. G. Efimov, and V. F. Stelmakh, *Nucl. Instrum. Methods Phys. Res. B* **69**, 271 (1992).

⁶Y. Lifshitz, Th. Kohler, Th. Frauenheim, I. Guzmán, A. Hoffman, R. Q. Zhang, X. T. Zhou, and S. T. Lee, *Science* **297**, 1531 (2002).

- 451 ⁷Y. Lifshitz, X. M. Meng, S. T. Lee, R. Akhvelidyan, and A.
 452 Hoffman, Phys. Rev. Lett. **93**, 056101 (2004).
 453 ⁸Sh. Michaelson and A. Hoffman, Diamond Relat. Mater. **14**, 470
 454 (2005).
 455 ⁹E. H. T. Tao, B. K. Tang *et al.*, Adv. Mater. (Weinheim, Ger.) (to
 AQ: #56 be published).
 10 457 ¹⁰G. Kopidakis, C. Z. Wang, C. M. Soukoulis, and K. M. Ho,
 458 Phys. Rev. B **58**, 14106 (1998).
 AQ: #59 ¹¹O. Ofer, J. Adler, and A. Hoffmann, Int. J. Mod. Phys. C **17**, 959
 11 460 (2006).
 461 ¹²K. Kohary, S. Kugler, Z. Hajnal, T. Köhler, T. Frauenheim, S.
 462 Kátai, and P. Deák, Diamond Relat. Mater. **11**, 513 (2002).
 463 ¹³M. M. M. Bilek, D. R. McKenzie, D. G. McCulloch, and C. M.
 Goringe, Phys. Rev. B **62**, 3071 (2000). **464**
¹⁴S. Iarlori, G. Galli, and O. Martini, Phys. Rev. B **49**, 7060 **465**
 (1994). **466**
¹⁵A. Sorkin, Joan Adler, and R. Kalish, Phys. Rev. B **74**, 064115 **467**
 (2006). **468**
¹⁶C. Z. Wang, K. M. Ho, and C. T. Chan, Phys. Rev. Lett. **70**, 611 **469**
 (1993). **470**
¹⁷J. Adler, A. Hashibon, N. Schreiber, A. Sorkin, S. Sorkin, and G.
 Wagner, Comput. Phys. Commun. **147**, 665 (2002). **471**
¹⁸C. Z. Wang and K. M. Ho, Phys. Rev. Lett. **71**, 1184 (1993). **473**
¹⁹A. P. Horsfield, Phys. Rev. B **56**, 6594 (1997). **474**
²⁰V. M. Titov, V. F. Anisichkin, and I. Yu. Mal'kov, Fiz. Goreniya **475**
 Vzryva **25**, 117 (1989). **476**

AUTHOR QUERIES —

- #1 Q1: AU: Please check if the changes made in the sentence “Most of these, except...” preserves your meaning.
- #2 Q2: AU: Please check if the change of “/” to “or”.
- #3 Q3: AU: Please check the insertion of Ref. 16 citation here.
- #4 Q4: AU: Please check if the inserted definition of “RAM” here preserves your meaning.
- #5 Q5: AU: Please check if the insertion of “and” here preserves your meaning.
- #6 Q6: AU: Please check if the insertion of “shown” here preserves your meaning.
- #7 Q7: AU: Please check the insertion of Ref. 6 citation here.
- #8 Q8: AU: PRB prefers not to make claims of novelty. Please check changes made in this sentence.
- #9 Q11: AU: Please be aware that although figure caption makes reference to color online, figures in print will still appear in black and white.
- #10 Q9: Au: Please supply full list of authors and please update.
- #11 Q10: CrossRef reports the volume should be '17' not 'V17' in the reference 11 'Ofer, Adler, Hoffmann, 2006'.